COMMISSION XV

DESIGN,

ANALYSIS AND

FABRICATION OF WELDED STRUCTURES

XV- 1410-12

MEMBRANE ACTION OF COMPOSITE STRUCTURES IN CASE OF FIRE

Author(s) JÁRMAI, Károly, VASSART, Olivier, ZHAO, Bin

Abstract:

Large scale fire tests conducted in a number of countries and observations of actual building fires have shown that the fire performance of composite steel framed buildings is much better than is indicated by fire resistance tests on isolated elements. It is clear that there are large reserves of fire resistance in modern steel framed buildings and that standard fire resistance tests on single unrestrained members do not provide a satisfactory indicator of the performance of such structures. There have been two European projects on membrane action, the FRACOF and the MACS+ projects. FRACOF concentrated on the theoretical background, simulations and measurements. MACS+ main activity is the dissemination of this knowledge. In both projects the coordinator was ArcelorMittal. This presentation is part of the dissemination project.

IIW Keywords:

fire safety, welded rebar mesh, composite structures, membrane action

Notes:[Notes]

Membrane action of composite structures in case of fire

Author(s) JÁRMAI, Károly, VASSART, Olivier, ZHAO, Bin

Author information JÁRMAI, Károly, University of Miskolc, Hungary, VASSART, Olivier, ArcelorMittal Esch, Research and Development, Luxembourg, ZHAO, Bin, CTICM –Fire and Testing Division, France

ABSTRACT

Large scale fire tests conducted in a number of countries and observations of actual building fires have shown that the fire performance of composite steel framed buildings is much better than is indicated by fire resistance tests on isolated elements. It is clear that there are large reserves of fire resistance in modern steel framed buildings and that standard fire resistance tests on single unrestrained members do not provide a satisfactory indicator of the performance of such structures. There have been two European projects on membrane action, the FRACOF and the MACS+ projects. FRACOF concentrated on the theoretical background, simulations and measurements. MACS+ main activity is the dissemination of this knowledge. In both projects the coordinator was ArcelorMittal. This presentation is part of the dissemination project.

IIW-Thesaurus keywords fire safety, welded rebar mesh, composite structures, membrane action:

1. CARDINGTON FIRE TEST PROGRAM

1.1 Research programme

In September 1996, a programme of fire tests was completed in the UK at the Building Research Establishment's Cardington Laboratory. The tests were carried out on an eight-storey composite steel-framed building that had been designed and constructed as a typical multi-storey office building. The purpose of the tests was to investigate the behaviour of a real structure under real fire conditions and to collect data that would allow computer programs for the analysis of structures in fire to be verified.


Figure 1.1 *Cardington test building prior to concreting of the floors*

The test building (see Figure 1.1) was designed to be a typical example of both the type of braced structure and the load levels that are commonly found in the UK. In plan, the building covered an area of 21 m × 45 m and had an overall height of 33 m. The beams were designed as simply supported, acting compositely with a 130 mm floor slab. Normally, a building of this type would be required to have 90 minutes fire resistance. Fin-plates were used for the beam-to-beam connections and flexible end plates for the beam-to-column connections. The structure was loaded using sandbags distributed over each floor to simulate typical office loading.

There were two projects in the research programme. One project was funded by Corus (formerly British Steel) and the European Coal and Steel Community (ECSC); the other was funded by the UK Government via the

Building Research Establishment (BRE). Other organisations involved in the research programme included Sheffield University, TNO (The Netherlands), CTICM (France) and The Steel Construction Institute. Fire tests took place between January 1995 and July 1996. The tests were carried out on various floors; the location of each test is shown on the floor plan in Figure 1.2.
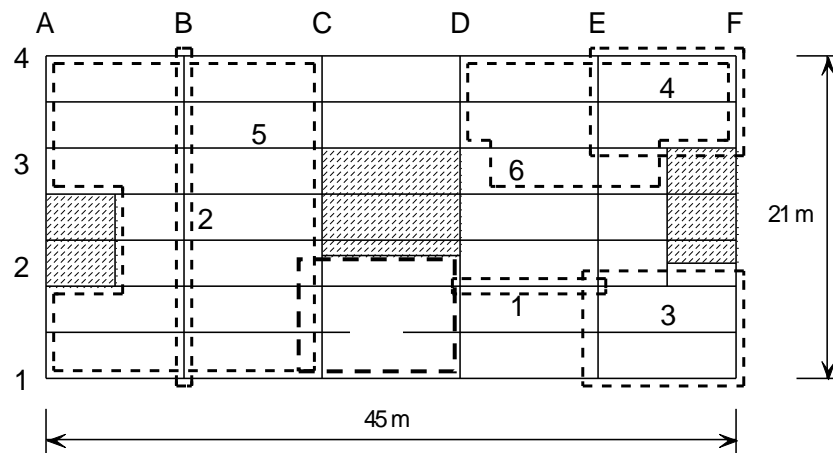
1. Restrained beam (ECSC)   4. Corner (BRE)
2. Plane frame (ECSC)   5. Large compartment (BRE)
3. Corner (ECSC)   6. Office demonstration (ECSC)
7. Central compartment (CTU)

Figure 1.2. *Test Locations*

Test 1 involved a single secondary beam and the surrounding floor slab, which was heated by a purpose-built gas-fired furnace. Test 2 was also heated using gas, and was conducted on a plane frame spanning across the building on one floor; the test included primary beams and associated columns. Tests 3, 4 and 5 involved compartments of various sizes subjected, in each case, to a natural fire fuelled by timber cribs. The columns in these tests were protected up to the underside of the floor slab and the beams and floor slab were left unprotected. Test 6 was a demonstration, which used furniture and contents typically found in modern offices as the fire load, leading to the most severe fire.

A detailed description of the tests has been published [1]. The complete test data, in electronic form with accompanying instrument location maps, is available for Tests 1, 2, 3 and 6 from Corus RD&T (Swinden Technology Centre) [2] and for Tests 4 and 5 from BRE [3,4].

2   DEVELOPMENT OF DESIGN GUIDANCE

Previous tests at normal temperature have shown that the load bearing capacity of concrete slabs will be enhanced by membrane forces provide that vertical support is maintained along the slab boundaries. Flat slabs, which only have vertical supports at their corners, do not develop significant tensile membrane forces and therefore benefit little from enhancement due to membrane action.

Therefore, for a composite slab supported on a grillage of steel beams in fire conditions, it is important to divide the slab into rectangular areas, referred to as floor design zones, where vertical support can be maintained on the perimeter of each area. These lines of vertical support are achieved by ensuring that the perimeter beams frame into column positions and are fire protected.

At ambient temperature, the floor is continuous over the boundary of each floor design zone. However, in fire conditions it is likely that cracks will form over the perimeter beams, due to the large thermal curvatures experienced by the slab. This may lead to fracture of the reinforcement, either due to the curvature or due to the combination of bending and membrane stresses. The fracture of the reinforcement in these hogging regions will occur before fracture of the reinforcement in the centre of the floor design zone. Therefore, the floor design zones are considered to have no rotational or transverse restraint along the boundary of the slab.

2.1 Design assumptions

For a composite floor slab, the yield line pattern will depend on the behaviour of the unprotected composite beams, which are continually losing strength as the temperature increases. Unlike ambient conditions the load carrying mechanism of the floor changes with increasing temperature. Initially, the composite slab acts as a one-way spanning element supported on the secondary beams. As these beams lose strength with increasing temperature and the behaviour of the slab tends to the behaviour of a simple supported two-way spanning element, resulting in the formation of the yield line pattern shown in Figure 2.1. By assuming that this ultimate failure condition will occur when the beam strength is low relative to the slab, a conservative estimate of capacity can be obtained relatively simply.

The load bearing capacity of the slab is calculated on the assumption that the composite beams have no strength and is based on the yield line pattern which is compatible with the boundary conditions and which provides the lowest load bearing capacity. This resistance is then enhanced by taking account of the tensile membrane effects based on the estimated deflection of the slab and the modes of failure. The bending resistance of the composite beams are added to this enhanced slab resistance in order to give the total load bearing capacity of the system.
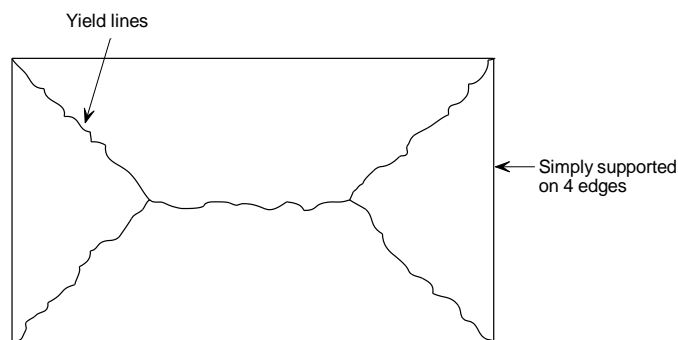

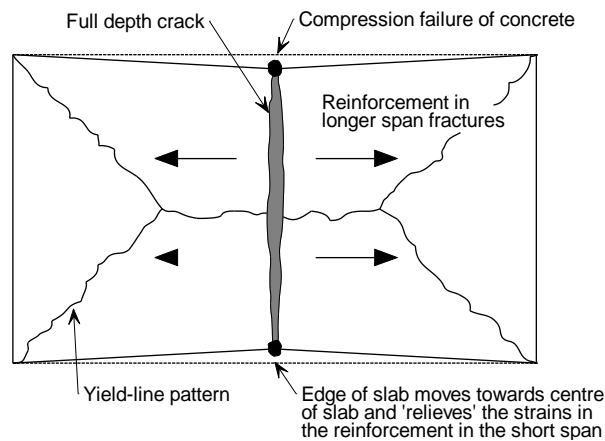Figure 2.1 *Typical yield line pattern for a rectangular slab simply supported along four edges*

Figure 2.2 *Tensile failure of the slab due to fracture of the reinforcement*

2.2 Failure criterion

Two modes of failure have been witnessed in room temperature and elevated temperature tests, depending on the reinforcement ratio, slab aspect ratio and the reinforcement ductility. Fracture of the reinforcement across the shorter span dominates the failure mode in most of the lightly reinforced slabs, whilst the heavily reinforced slabs and slabs with highly ductile reinforcement may experience compressive failure at the corners of the slab. Both modes of failure are considered by the simple design method.

Most tests conducted at elevated temperatures on simply supported concrete slabs have failed due to full depth crack forming across the shorter span (l), as shown in Figure 2.2. The design method predicts the load bearing

capacity for a given deflection. This Chapter describes the development of an expression for estimating slab deflection just prior to slab failure which is required to calculate the effect of membrane action.

2.2.1   Slab deflection

As the simple design method is based on plastic theory, deflection cannot be calculated using the method. However, in order to calculate the membrane forces a value of deflection for the slab just prior to failure must be estimated. This estimate of slab deflection will include thermal strains due to the slabs temperature gradient as well as the mechanical strains in the reinforcement.

2.2.1.1   *Thermal effects*

Based on the previous investigations, when the maximum deflection of the slab is greater than almost 0.5 times its depth and tensile forces start to build up at the slab centre, any in-plane restraint to the thermal expansion would increase the vertical displacements (i.e. the slab is in the post-buckling phase) and therefore the tensile membrane action. Conservatively, and in order to allow this approach to be used also for the edge slabs, this beneficial effect is ignored and slab is assumed to be unrestrained.

The composite slab in the fire conditions would experience thermal curvature, which, for an unrestrained slab, increases the vertical displacement without inducing any mechanical strains into the mesh reinforcement. If the temperature distribution through the slab is assumed to be linear then the displacements caused by the thermal deflection is calculated as:

$$\frac{d^2 w}{dx^2} = \frac{\alpha(T_2 - T_1)}{h}$$

where

    w =Vertical displacement

    α = Coefficient of thermal expansion

    T_2 =Bottom temperature

    T_1 = Top temperature

    h = Depth of slab

The vertical displacement of the slab due to thermal curvature can be obtained by integrating the above Equation, which gives:

$$w_\theta = \frac{\alpha(T_2 - T_1)l^2}{8h}$$

where l is the length of the shorter span of the slab

This formulation is based on a constant atmospheric temperature throughout the fire compartment. To the estimated displacement, allowing for real fire conditions where uniform heating is less likely, a reduction factor of 2.0 is applied to the above expression. This results in the design value of vertical displacement due to the thermal curvature given by:

$$w_\theta = \frac{\alpha(T_2 - T_1)l^2}{16h}$$

2.2.1.2   *Mechanical strains in the reinforcement*

Assuming that the deflected shape of the slab due to transverse loading is parabolic, the length of the deflected slab is given by the following formulation in which the longer span is (L).

$$L_c = L\left(1 + \frac{8w^2}{3L^2} - \frac{32w^4}{5L^4} + \ldots\ldots\right)$$

where L_c is the length of the curve, L is the length of longer span of slab at zero displacement, w is the vertical displacement of the curve.

For flat curves,

$$L_c = L\left(1 + \frac{8w^2}{3L^2}\right)$$

Hence, the strain in the mesh can be calculated by:

$$\varepsilon = \frac{8w^2}{3L^2}$$

This equation assumes the strain is the same value along the length of the slab. In reality, the slab will experience tension stiffening with strains being concentrated where cracks have occurred. The reinforcement across a crack will also experience a significant increase in the strain, resulting in the eventual fracture of the reinforcement. Therefore, to allow for tension stiffening the component of displacement due to strain in the reinforcement w_ε is based on a conservative value of average strain calculated at a stress equal to half the yield stress at room temperature. The displacement is then given by:

$$w_\varepsilon = \sqrt{\left(\frac{0.5 f_{sy}}{E_s}\right) \frac{3L^2}{8}}$$

(1)

where E_s is the room temperature elastic modulus of the reinforcement

f_{sy} is the room temperature yield strength of the reinforcement

The displacements due to strain in the reinforcement calculated using Equation (1) have been compared to maximum deflections measured in tests at room temperature. In all the cases considered, the displacement predicted by Equation (1) was lower than the maximum displacement recorded in the test, as shown in Table 2.1.

Table 2.1 *Comparison of allowable deflection from Equation (1) and maximum deflections measured in room temperature tests.*

Test	Slab size (m)	Effective Depth (mm)	Reinforcement Diameter (mm)	Bar Spacing (mm)	Steel yield strength (N/mm²)	Max. test deflection (mm)	Allowable deflection Eqn. (1) (mm)
BRE	9.56x6.46	66.0	6.0	200	580	223	216
Sawczuk & Winnicki	1.6x1.1	26.0	3.0	30.0	263	127*	25
	2.0x1.0	26.0	3.0	60.0	263	76*	31
Hayes & Taylor	0.914x0.914	15.9	9.5	-†	505	50.8*	19.4
	0.914x1.372	15.9	9.5	-†	505	50.8*	29.1
	0.914x1.829	15.9	9.5	-†	505	50.8*	38.8
Taylor, Maher & Hayes	1.829x1.829	43.6	4.8	76.2	376	81	33.5
	1.829x1.829	37.3	4.8	63.5	376	98	33.5
	1.829x1.829	69.0	4.8	122	376	84	33.5
Brothie & Holley	0.381x0.381	14.2	2.3	-†	414	11.6	7.32
	0.381x0.381	31.0	3.4	-†	379	7.45	7.0

*test terminated before fracture of the reinforcement

† Data not reported

2.2.1.3   *Calculation of slab deflection to allow the calculation of membrane forces*

The tensile membrane action of the slab is then calculated based on a slab displacement estimated by combining the components due to thermal curvature and strain in the reinforcement, resulting in:

$$w_m = \frac{\alpha(T_2 - T_1)l^2}{16h} + \sqrt{\left(\frac{0.5 f_{sy}}{E_s}\right) \frac{3L^2}{8}}$$

(2)

This equation results in a conservative estimate of load bearing capacity since:

- the estimated vertical displacements due to thermal curvature are divided by two.

- the thermal curvature is calculated based on the shorter span of the slab

- any additional vertical displacements induced by the restrained thermal expansion when the slab is in a post buckled state are ignored

- any contribution from the steel decking is ignored

- the increase of the mesh ductility with the temperature increase is ignored.

2.2.2 Calibration against Cardington fire tests

Bailey & Moore [5] demonstrated that the design method provided a reasonable prediction of floor slab capacity when compared to the Cardington Fire Tests. As part on this project a further furnace based fire test has been conducted.

The above expression for slab deflection was compared to the maximum deflections recorded during the Cardington fire tests. The object was to ensure that the deflections estimated would be conservative when compared to actual slab behaviour just prior to failure. The drawback in using these tests for this purpose was that failure was not reached by the slabs tested therefore the maximum measured deflections do not correspond to failure of the slab. However, it is known that the results of the comparison will be conservative but the degree of conservatism cannot be quantified.

Table 2.2 shows the comparison between the limiting deflection given by Eq. (2) and the maximum measured deflection from each of the Cardington tests. This comparison includes both thermal and mechanical strains, which are impossible to distinguish in test data.

In all cases, Equation (2) gives deflections which are greater than the measured deflections. In order to ensure that the deflection limit is conservative Bailey and Moore [6] limited the deflection to those recorded in the tests.

Table 2.2 *Comparison of the displacement given by Equation (2) against the maximum displacements recorded in the six Cardington fire tests.*

Test	L	l	Deflection due to thermal curvature	Deflection due to mechanical strain (mm)	Deflection limit Eqn. (2)	Maximum deflection recorded in test	Deflection Limit/test deflection
	(m)	(m)	(mm)		(mm)	(mm)	
BRE Corner Test	9.0	6.0	135	208	343	269	1.28
British Steel Restrained Beam	9.0	6.0	135	208	343	232	1.50
British Steel 2-D test	14.0	9.0	0*	324	324	293	1.11
BS Corner Test	10.223	7.875	231	237	468	428	1.09
BRE Large Compartment Test	21.0	9.0	303	486	789	557	1.42
BS Office Demo Test	14.6	10.0	373	338	711	641	1.11

*Due to the small area of slab heated in this test the displacement due to thermal curvature was taken as zero.

For mechanical strains, Bailey and Moore introduced an additional limit as shown below.

$$w_\varepsilon = \sqrt{\left(\frac{0.5f_y}{E}\right)_{re\inf} \frac{3L^2}{8}} \text{ but } w_\varepsilon \leq \frac{l}{30}$$

For thermal deflection they also increased the 'factor of safety' from 2 to 2.4 giving the following conservative expressions for estimating slab deflections:

$$w_m = \frac{\alpha(T_2 - T_1)l^2}{19.2h} + \sqrt{\left(\frac{0.5f_{sy}}{E_s}\right)\frac{3L^2}{8}} \tag{3}$$

but not more than $\dfrac{\alpha(T_2 - T_1)l^2}{19.2h} + \dfrac{l}{30}$

Table 2.3 *Comparison of the displacement given by Equation (3) against the maximum displacements recorded in the six Cardington fire tests.*

Test	L (m)	l (m)	Deflection due to thermal curvature (mm)	Deflection due to mechanical strain (mm)	Deflection limit Eqn. (3) (mm)	Maximum deflection recorded in test (mm)	Deflection Limit/test deflection
BRE Corner Test	9.0	6.0	112	200	312	269	1.16
British Steel Restrained Beam	9.0	6.0	112	200	312	232	1.34
British Steel 2-D test	14.0	9.0	0*	300	300	293	1.02
BS Corner Test	10.223	7.875	193	237	430	428	1.00
BRE Large Compartment Test	21.0	9.0	252	300	552	557	0.99
BS Office Demo Test	14.6	10.0	311	333	644	641	1.00

*Due to the small area of slab heated in this test the displacement due to thermal curvature was taken as zero.

Table 2.3 shows the comparison between the limiting deflection given by Equation (3). Given that failure did not occur in any of the tests it was felt that it would be overly conservative to reduce the deflection limit to a point where the ratio of deflection limit to measured deflection was one for all tests. For the large compartment tests this limit appears to be reasonable.

2.3 Design methodology

The design methodology advocated in this document is based on two key principles.

- The risk to life safety of the building occupants, fire fighters and others in the vicinity of the building in the event of a fire should not increase relative to current practice as a result of using the method.

- The fire should be contained within its compartment of origin and the application of the design method should not lead to failure of the compartmentation of the building

The design method is intended to apply to composite steel-concrete floor plates supported on composite or non-composite columns. The structural frame should be braced (non-sway), the connections should be simple nominally pinned connections and the concrete floor slab should be constructed using steel decking not exceeding 80 mm in depth and supported on the top flange of the steel section. The steel beams should be designed to act compositely with the floor slab in accordance with the recommendations of EN 1994-1-1 [13]. Excluded from the scope of application are slabs with an exposed concrete soffit including precast concrete slabs and beams with multiple web openings.

In order to apply the simple design method to a design scenario, the floor plate being considered must be divided into a number of 'floor design zones'. These floor design zones are bounded on their perimeters by beams (normally fire protected) which satisfy the fire resistance requirements specified for the floor plate. Each floor design zone may include a number of internal secondary beams without fire protection which have a much lower fire resistance. The provision of protected beams on the perimeter of the floor slab is intended to result in slab behaviour in keeping with the assumption that the perimeter of the floor design zone is simply supported.

For periods of fire resistance of 60 minutes or above the perimeter of the floor design zones should correspond to the column gridlines and the perimeter beams should be connected to the columns at either end.

The composite slab may be designed in accordance with EN 1994-1-1 and should also satisfy the minimum insulation thickness recommended by EN 1994-1-2 [11] in fire conditions. Reinforcement of the composite slab should be achieved using a steel mesh. Reinforcement in the ribs of the slab is not considered in the design method. The inclusion of such reinforcement can have a negative as well as a positive effect on the slab performance in fire conditions, as compressive failure in the concrete may result if the slab is over reinforced.

2.3.1 Calculation of load bearing capacity for unprotected beams

In fire conditions, the unprotected beams within each floor design zone will add to the tensile resistance of the slab via catenary action.

The temperature of the cross-section of the unprotected beams is calculated using the method given in EN 1994-1-2, 4.3.4.2.2. The bottom flange, the web and the top flange of the steel profile are assumed to be at have each a uniform temperature for the calculation of the moment resistance.

The calculation of the plastic moment resistance of the beams at elevated temperature follows the principles of EN 1994-1-2, 4.3 taking account of the degree of shear connection between the steel section and the concrete. The temperature of the slab is taken as 40 % of the temperature of the top flange

For the plain profiles, the complete steel profile is taken into account. For the Cellular beams, the test performed in Ulster showed that after the web post buckling of the Cellular Beam, it is not relevant to take into account the plastic resistance of the complete beam. So after the Web post buckling of the Cellular Beam, in order to be safe sided, only the tension appearing in the upper tee of the section will be taken into account.
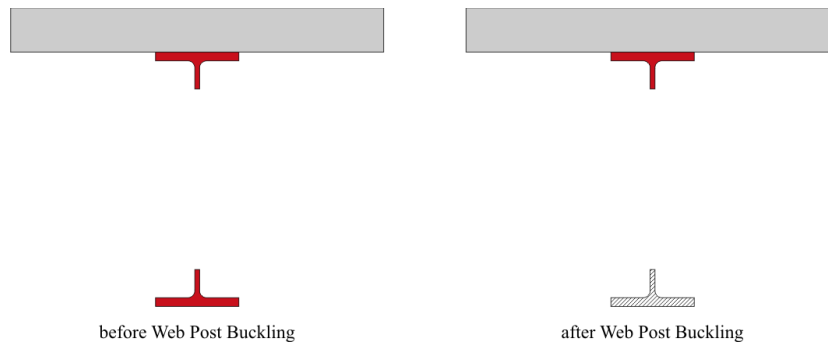

before Web Post Buckling   after Web Post Buckling

Figure 2.3.: *Steel section before and after Web Post Buckling*

In order to implement that in the analytical method and to ensure the transition between the complete Cellular Beam profile and the Cellular Beam after the web post buckling, a new material law has been developed for the steel of the lower member.

2.4 Design of fire resisting perimeter beams

The perimeter beams which bound each floor design zone must be designed to achieve the period of fire resistance required by the floor slab. This will ensure that the pattern of yield lines and the associated enhancement due to tensile membrane action which are assumed to occur in the design methodology actually occur in practice. The required moment resistance of the edge beams is calculated by considering alternative yield line patterns that would allow the slab to fold along an axis of symmetry without developing tensile membrane action, as shown by Figure 2.3 and Figure 2.4.
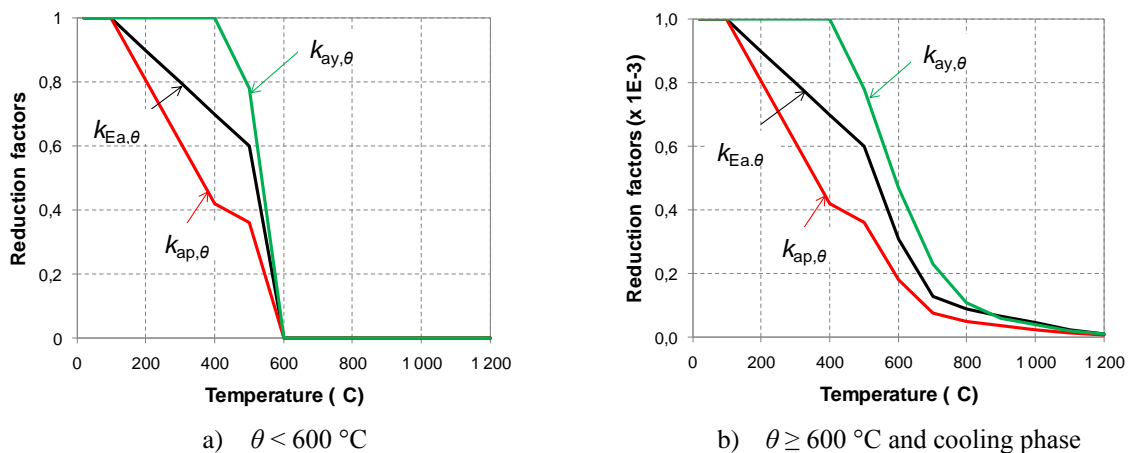

a) $\theta < 600\ °C$ b) $\theta \geq 600\ °C$ and cooling phase

Figure 2.4 : *Reduction factors of structural steel in unprotected cell beam lower tee*

Having calculated the required moment capacity of these beams to ensure that they provide sufficient support to allow development of the tensile membrane enhancement of the slab load bearing resistance, a critical temperature for the beams can be calculated and appropriate levels of fire protection can be applied to ensure that this critical temperature is not exceeded during the required fire resistance period.
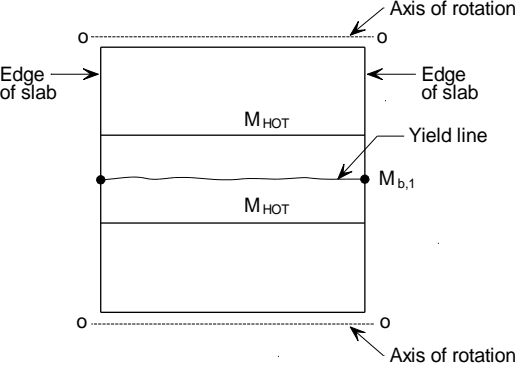

Figure 2.5 *Alternative yield line patterns involving the formation of plastic hinges in the perimeter beams*

The design method assumes that an envelope pattern of yield lines will form in the slab at the ultimate limit state. In order for this to occur, the beams on the perimeter of the floor design zone must have sufficient moment resistance to prevent a beam and slab mechanism occurring at a lower load level.

For a typical floor design zone, as shown in Figure 2.5 and 2.6, two yield line patterns have been considered which include the formation of a plastic hinge in the perimeter beams. The yield lines may occur across the centre of the slab, either parallel to the unprotected beams in the Span 1 direction with plastic hinges forming in the perimeter beams on Sides A and C or perpendicular to the unprotected beams in the Span 2 direction with plastic hinges forming in the perimeter beams on Side B and D and in the unprotected beams.
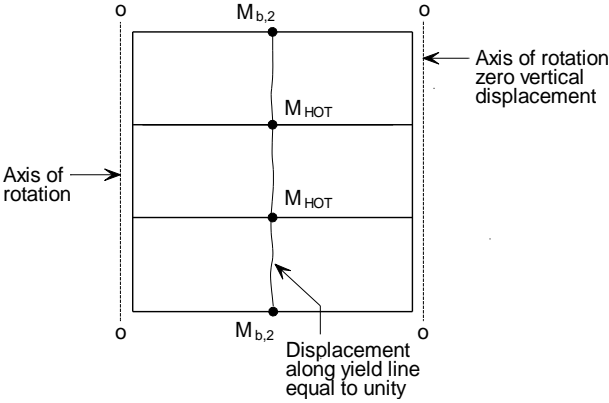

Figure 2.6 *Alternative yield line patterns involving the formation of plastic hinges in the perimeter beams*

Using this pattern of yield lines and equating the internal and external work for the mechanism, the moment resistance of the perimeter beams required to achieve a load bearing capacity equal to that for the floor slab may be determined. The derivation of appropriate design equations is given below.
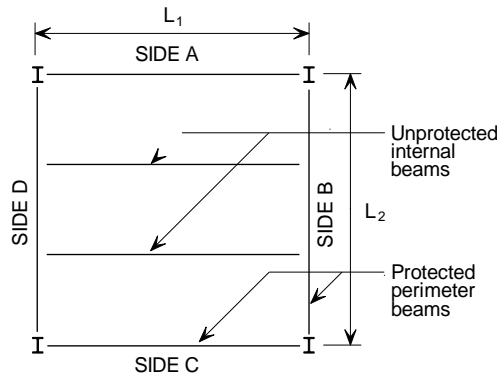
Figure 2.7 *Typical floor design zone*

2.4.1 Unprotected beams with edge beams on both sides

2.4.1.1 *Yield line parallel to unprotected beams*

This case considers the required moment resistance of the perimeter beams on Sides B and D of the floor design zone. These beams are also assumed to be at the edge of the slab. A single yield line is assumed to form across the centre of the floor design zone in the Span 1 direction, as shown in Figure 2.6. In keeping with the assumptions of the design method the perimeter of the floor design zone is assumed to be simply supported.
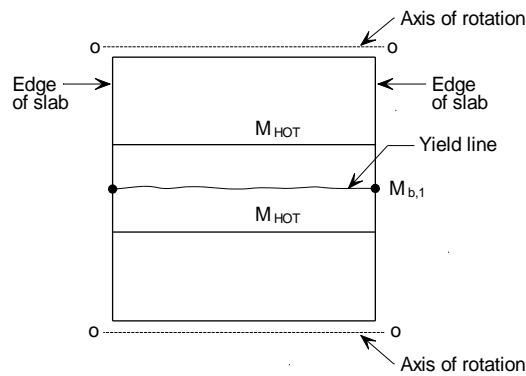

Figure 2.8 *Yield line in parallel to the unprotected beams edge condition on Sides B and D*

Considering a unit displacement along the yield line, the rotation of the yield line can be calculated as follows:

Yield line rotation $= 2\dfrac{1}{L_2/2} = \dfrac{4}{L_2}$

The internal work done due to the rotation of the yield line is given by:

Internal Work $= \left(ML_{1,\text{eff}} + 2M_{b,1}\right)\dfrac{4}{L_2} = \dfrac{4M\,L_{1,\text{eff}}}{L_2} + \dfrac{8M_{b,1}}{L_2}$

where

$L_{1,\text{eff}}$ is the effective length of the yield line discounting the effective width of slab assumed to act with the perimeter beams where these are design as composite members.

M is the moment resistance of the slab per unit length of yield line

For a uniform load on the slab, *p*, the external work due to the displacement is given by:

External Work $= \dfrac{1}{2}pL_1L_2$

Equating internal and external work gives:

$$pL_1 L_2 = \frac{8ML_{1,\text{eff}}}{L_2} + \frac{16M_{\text{b},1}}{L_2}$$

If the load on the slab is the load bearing capacity, the required minimum values of moment resistance for the perimeter beams on Side B and D is given by:

$$M_{\text{b},1} = \frac{pL_1 L_2^{\ 2} - 8ML_{1,\text{eff}}}{16}$$

where

p is the uniformly distributed load to be supported by the floor design zone in fire conditions.

2.5   Thermal Analysis

The FRACOF software [17,18] uses a 2D finite difference heat transfer method to predict the temperature distribution within the composite slab. This method has been used for many years by SCI to predict the temperature distributions in steel and steel-concrete composite cross sections and has been shown to be able to reasonably predict the behaviour of sections in fire resistance tests.

The object to be analysed must defined on a rectangular grid of cells. The method can also analyse the sloping sides of trapezoidal or re-entrant composite slabs by using configuration factors given below.

The thermal properties of steel and concrete used by the FRACOF software are based on the values given by EN1994-1-2.

The thermal actions are calculated on the basis of the net heat flux, $\dot{h}_{\text{net}}$ to which the surface of the member is exposed. The net heat flux is determined considering the heat transfer by convection and radiation.

$$\dot{h}_{\text{net}} = \dot{h}_{\text{net,c}} + \dot{h}_{\text{net,r}} \tag{4}$$

The net convective heat flux component is determined as follows:

$$\dot{h}_{\text{net,c}} = \alpha_{\text{c}} \left(\theta_{\text{g}} - \theta_{\text{m}} \right) \tag{5}$$

where α_{c} is the coefficient of heat transfer by convection

        θ_{g} is the gas temperature

        θ_{m} is the surface temperature of the member

When carrying out a thermal analysis for a member exposed to the standard temperature –time curve the coefficient of heat transfer by convection on the exposed face is taken as $\alpha_{\text{C}} = 25$ W/m^{2}K.

For natural fire models the coefficient of heat transfer by convection is increased to $\alpha_{\text{C}} = 35$ W/m^{2}K.

On the unexposed side of the slab the net heat flux is based on heat transfer by convection , but the coefficient of heat transfer by convection is taken as $\alpha_{\text{C}} = 9$ W/m^{2}K, to allow for the effects of heat transfer by radiation which are not considered explicitly in the model.

The net radiative heat flux is determined from the following formula

$$h_{\text{net,r}} = \Phi \varepsilon_{\text{m}} \varepsilon_{\text{f}} \ \sigma \left[\left(\theta_{\text{r}} + 273 \right)^4 - \left(\theta_{\text{m}} + 273 \right)^4 \right] \tag{6}$$

where Φ is the configuration factor

        ε_{m} is the surface emissivity of the member

        ε_{f} is the emissivity of the fire

        σ is the Stephan Boltzmann constant (5,67 x 10^{-8} W/m^{2}K^4)

        θ_{r} is the effective radiation temperature of the fire

        θ_{m} is the surface temperature of the member

The emissivity of the fire is taken as $\varepsilon_f = 1.0$ in accordance with the recommended value in EN1994-1-2. The emissivity of the member may be determined from 0.

2.5.1 Configuration Factors

For steel decking profiles the following configuration factors are used to modify the net heat flux incident on each surface. The locations in which the following factors are applied are shown in Figure 2.7 for trapezoidal deck profiles and in Figure 2.8 for re-entrant deck profiles.

Trapezoidal Profiles

The bottom flange of the trapezoidal profile is assumed to have a configuration factor of 1.0. For the top flange the configuration factor, Φ_{TOP}, is calculated as follows.

$$\Phi_{TOP} = \frac{2\tan^{-1}\left(\dfrac{h}{2(p - b_1)}\right)}{3.14}$$

Similarily for the sloping web of the trapezoidal profile, the configuration factor, Φ_{SIDE}, is calculated as follows,

$$\Phi_{SIDE} = 0.5\frac{L}{x + y}$$

Re-entrant Deck

The bottom flange of re-entrant steel profiles is assumed to have a configuration factor of 1.0. The configuration factor for the surfaces of the re-entrant dovetail is calculated as follows,
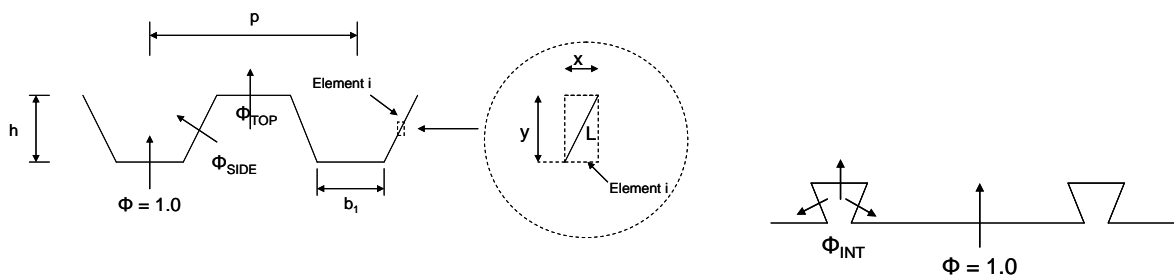
$$\Phi_{INT} = 0.3\frac{L}{x + y}$$

Figure 2.9a *Configuration Factors for trapezoidal decks* Figure 2.9b *Configuration Factors for re-entrant decks*

2.5.2 Material Properties

The following material properties are used for steel and concrete. These values are based on the recommendations of EN1994-1-2. 0 shows the values of surface emissivity, density and moisture content used for steel, normal weight concrete and light weight concrete.

Table 2.4 *Material properties for steel and concrete*

	Steel	NWC	LWC
Emissivity, ε_m	0.7	0.7	0.7
Density, ρ	7850	2300	1850
% moisture by mass	0	4	4

The specific heat capacity of steel, C_a, for all structural and reinforcing steel is given by the following temperature dependant formulae:

$$C_a = 425 + 0.773\theta - 0.00169\theta^2 + 0.00000222\theta^3 \quad \text{(J/kg K)} \qquad \text{for } 20°C \leq \theta \leq 600°C$$

$$C_a = 666 - \frac{13002}{(\theta - 738)} \quad \text{(J/kg K)} \qquad \text{for } 600°C \leq \theta \leq 735°C$$

$$C_a = 545 - \frac{17820}{(\theta - 731)} \quad \text{(J/kg K)} \qquad \text{for } 735°C \leq \theta \leq 900°C$$

$$C_a = 650 \quad \text{(J/kg K)} \qquad \text{for } 900°C \leq \theta \leq 1200°C$$

The following temperature dependant values of specific heat capacity, C_c, are used for normal weight dry concrete with siliceous of calcareous aggregates.

$$C_c = 900 \quad \text{(J/kg K)} \qquad \text{for } 20°C \leq \theta \leq 100°C$$

$$C_c = 900 + (\theta - 100) \quad \text{(J/kg K)} \qquad \text{for } 100°C \leq \theta \leq 200°C$$

$$C_c = 1000 + (\theta - 200)/2 \quad \text{(J/kg K)} \qquad \text{for } 200°C \leq \theta \leq 400°C$$

$$C_c = 1100 \quad \text{(J/kg K)} \qquad \text{for } 400°C \leq \theta \leq 1200°C$$

As recommended by EN1994-1-2 the following temperature independent value of specific heat capacity is assumed for lightweight concrete.

$$C_c = 840 \quad \text{(J/kg K)} \qquad \text{for all temperatures}$$

The thermal conductivity of steel is defined using the following temperature dependent relationship.

$$\lambda_a = 54 - 0.033(\theta - 20) \qquad \text{but not less than 27.3} \qquad \text{(W/mK)}$$

For normal weight concrete the upper limit of thermal conductivity as defined by EN1994-1-2 has been used. The thermal conductivity for normal weight concrete is determined from the following temperature dependent relationship.

$$\lambda_C = 2 - 0.2451(\theta/100) + 0.0107(\theta/100)^2 \qquad \text{(W/mK)}$$

The thermal conductivity of lightweight concrete is also temperature dependent and is given by the following formula.

$$\lambda_C = 1 - (\theta/1600) \qquad \text{but not less than 0.5} \qquad \text{(W/mK)}$$

2.5.3   Internal heat transfer by conduction

The thermal analysis computes the conducted heat transfer between a cell and the four cells above, below and to the sides (Figure 2.9). No other cells are involved.
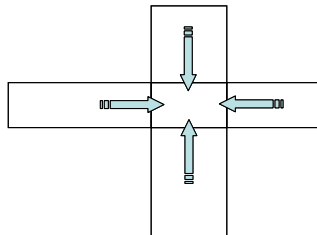

Figure 2.10 *Basis of conductive heat transfer*

The heat transferred per unit time depends on the sizes of the cells, the temperature of each cells and the thermal conductivity of each cell. Each pair of cells are considered in turn and the net heat transferred into or out of a cell is computed. The basic conduction model is illustrated in Figure 2.10.
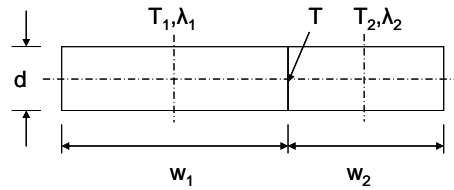

Figure 2.11 *Basic conduction model*

The temperature of each cell is defined at its centre (T_1, T_2). The temperature of the interface between the cells is T. The heat transfer from cell 1 to the interface is the same as the heat transfer from the interface to cell 2. The thermal conductivities of each cell are λ_1 and λ_2.

The heat transfer per unit time from the centre of cell 1 to the interface is:

$$h = \frac{2D\lambda_1}{w_1}(T - T_1)$$

This is equal to the heat transfer per unit time from the interface to the centre of cell 2:

$$h = \frac{2D\lambda_2}{w_2}(T_2 - T)$$

Thus, by eliminating the interface temperature, *T*:

$$h = \frac{(T_2 - T_1)}{\left(\dfrac{w_1}{2D\lambda_1} + \dfrac{w_2}{2D\lambda_2}\right)} \quad \text{per unit time}$$

This equation is used to compute the heat transfer between all cells. For each cell, the value of:

$$\frac{w}{2D}$$

is precalculated. The value of thermal conductivity will often vary with temperature and is calculated at preset intervals (normally 30 seconds) to speed up computation.

2.5.4   Design temperatures for unprotected steel beams

The design temperature of the unprotected steel beams are calculated based on the simple method given in EN1994-1-2 Section 4.3.4.2.2. The increase in steel temperature during a small time interval is calculated using the following equation.

$$\Delta\theta_{a,t} = k_{\text{shadow}}\left(\frac{1}{c_a \rho_a}\right)\left(\frac{A_i}{V_i}\right)\dot{h}_{\text{net}}\,\Delta t$$

where

k_{shadow} is the correction factor for shadow effect

ρ_a is the density of the steel

Δt is the time interval

A_i / V_i is the section factor for part i of the cross section

The FRACOF software calculates the steel temperature for the bottom flange of the section for time increments of 2.5 seconds. The correction factor for the shadow effect is taken as 1.0.

The section factor for the bottom flange is expressed as a function of flange thickness, e_1, as follows

$$A_i / V_i = \frac{2000}{e_1}$$

The net heat flux is calculated as shown in Equation (4), with the convective and radiative components calculated as shown by Equations (5) and (6) respectively. When calculating the radiative heat flux using Equation (6) the configuration factor should be taken as 1.0.

3 FULL-SCALE FIRE TEST ON A COMPOSITE FLOOR SLAB INCORPORATING LONG SPAN CELLULAR STEEL BEAMS

3.1 Test specimen

The tested floorplate was 9.6m by 15.6m supported on a steel frame spanning 9m by 15m between four corner columns (Figure 3.1). The cellular beams were positioned on gridlines 1, 4, B, C and D as primary and secondary beams of the structure (Figure 3.2). The dimensions of the beams are shown in Figure 3.3a and Figure 3.3b. The unprotected secondary Beams 4 and 5 also had an elongated web opening at the centre of their span.

Figure 3.1. Test compartment with long unprotected cellular beams
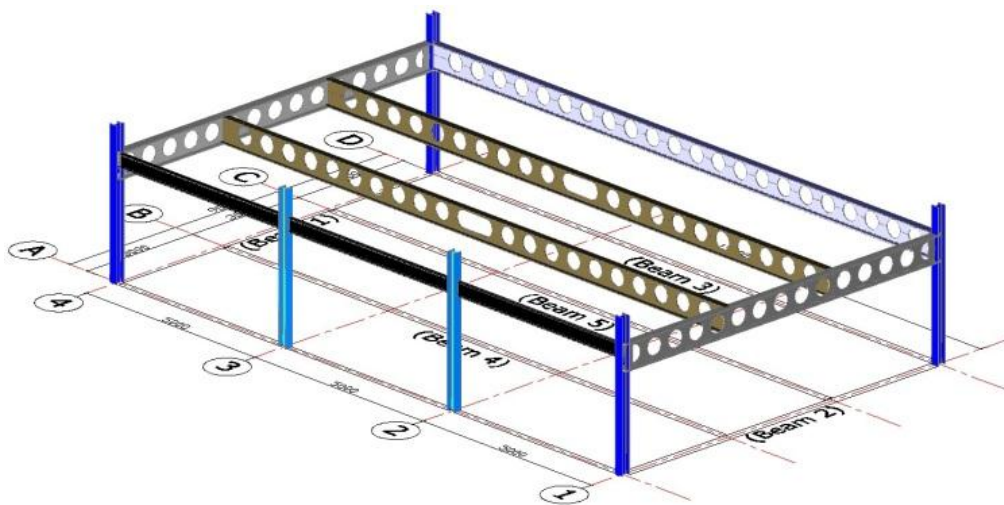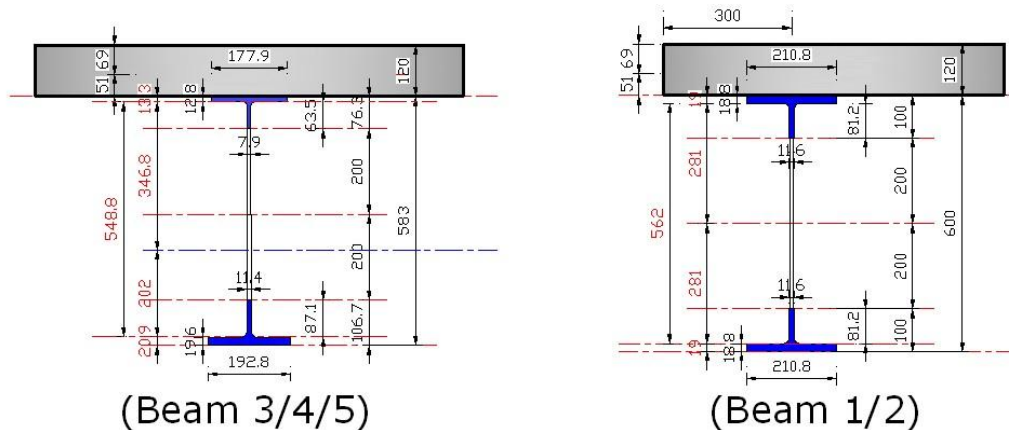

Figure 3.2. Steel structural layout

Figure 3.3a,b. Detail information of the steel sections.

The enclosed compartment was 9.2m by 15.6m, with an internal floor to soffit height of 2.88m. The surrounding walls were constructed using 7N/mm2 blockwork, with three openings, each 1.5m by 3m. The surrounding compartment walls along gridlines 1, 4 and D were not fixed to the composite floor at the top which allowed free vertical movement of the floorplate along these boundaries. The front façade, with openings, was constructed such that the wall was extended up to the underside of the solid beam along gridline A, allowing no vertical deflection of the beam along this gridline. The frame was braced in the horizontal direction at the following locations; Column A1 was braced in both lateral directions, Column A4 was braced laterally parallel to gridline 4 and Column D1 was braced laterally parallel to gridline D. Bracing was provided using a diagonal CHS.

All the columns, and the solid beam along gridline A, were protected using commercially available 20mm thick fire board with a standard fire resistance period of 2 hours. The perimeter CBs on gridlines 1, 4, and D were protected using a ceramic fibre, which also provided a standard fire resistance period of 2 hours. The fire protection was fitted using an approved contractor, following the manufacturer's specification. Plasterboard, 15mm thick, was also used to cover the inner face of the boundary walls to reduce heat loss through the blockwork.

Figure 3.4 Fibre and plasterboard protection used inside the compartment

The concrete composite slab was 120mm thick and comprised a 51mm deep, 1mm thick, Holorib steel deck (HR51/150), normal-weight concrete and mesh steel reinforcement. The dovetail steel deck had a measured tensile strength of $327N/mm^2$. The welded wire A393 mesh reinforcement (Figure 3.4) comprised 10mm diameter ribbed bars at 200mm centres, with nominal yield strength of $500N/mm^2$, which was specified using the Bailey Method [3], based on the design parametric fire curve. The mesh reinforcement had a minimum lap length of 400mm and covered with 40mm thickness of concrete. The concrete mix design (for 1m³) comprised: 320kg OPC, 918kg 10mm limestone, 691kg sharp sand, 380kg 6mm limestone, 30kg grey (recycled) water and 142kg cold (tap) water. No additives or air entraining agent was used in the concrete mixture. The measured average concrete compressive cube strength was $50N/mm^2$ on the day of test.
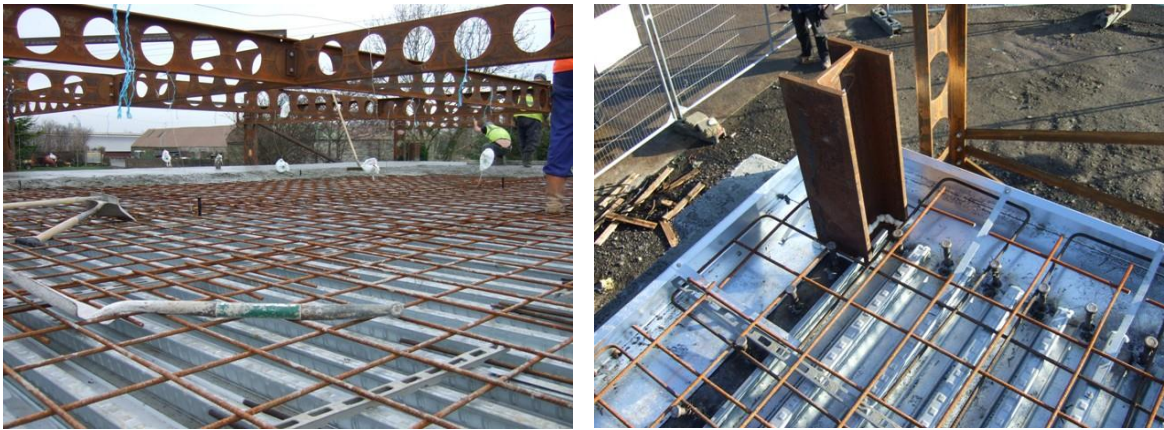

Figure 3.5. Mesh reinforcement and steel decking before concrete casting

Full interaction between the slab and beams was achieved using shear connectors, of 19mm diameter and 95mm height, placed at 200mm centres along the beams. The requirement for U-bar reinforcement around the slab's perimeter (as shown in Figure 3.5) is not a special requirement for fire design, but was needed to ensure correct reinforcement detailing for ambient design. The U-bars were 10mm diameter and placed with 30mm cover to the edge of the slab, as shown in Figure 3.5.

Design Loads

The design load was based on a characteristic live load of $3.5kN/m^2$ together with a partition load of $1.0kN/m^2$ and a services and finishes load of $0.5kN/m^2$. The partial load factors used for the Fire Limit State (FLS) correspond to the values given in the EN1990 for office buildings. The resulting applied load was $3.25kN/m^2$, as shown in Table 2.5.

Table 2.5 Design Loads

Description	Characteristic Load(kN/m^2)	Load Factor at FLS	Design Load at FLS kN/m^2
Partition	1.0	1.0	1.0
Services & Finishes	0.5	1.0	0.5
Live Load	3.5	0.5	1.75
		Total	**3.25**

The applied load was achieved using 44 sandbags (each weighting 1 tonne) evenly positioned over the floorplate, as shown in Figure 3.6a, providing a load of $3.25kN/m^2$. The self weight of the slab, which was 120mm thick, was calculated as $2.90kN/m^2$, creating a total load of $6.15kN/m^2$.

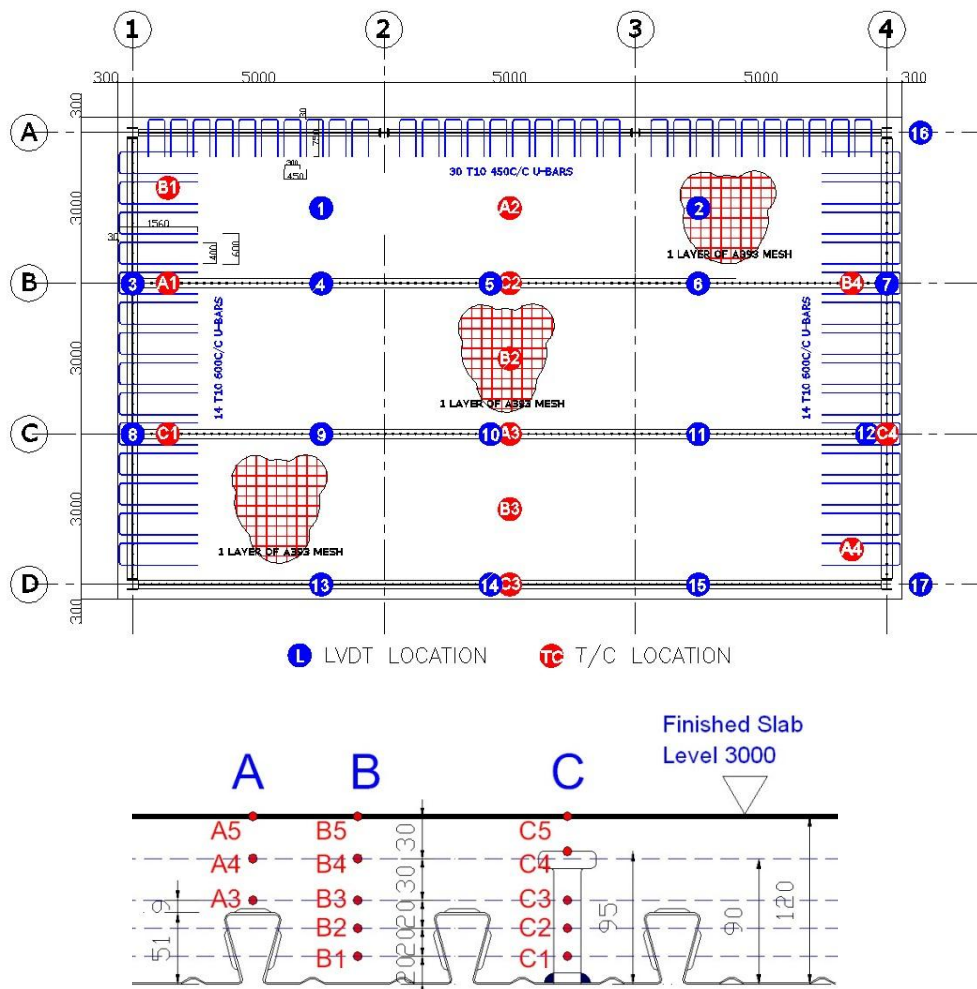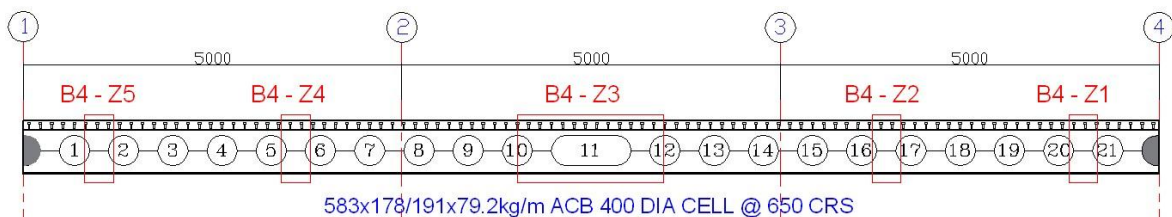Figure 3.6: (a)Vertical static load, (b)Wooden cribs used for the fire load

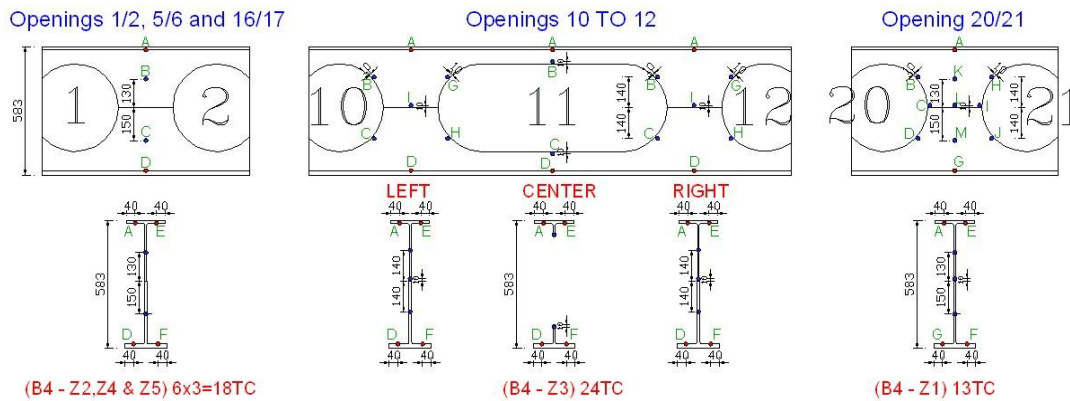Figure 3.7: Locations of measurement positions for deflections and temperatures throughout the slab.

Figure 3.8: Thermocouple locations on unprotected Beam 4 (Gridline B)

Design of the Fire

The natural fire was designed using the parametric time-temperature curves in Annex A of EN1991-1-2 and OZone Software. The fire load comprised 45 standard (1m x 1m x 0.5m high) wooden cribs, built using 50mm x 50mm x 1000mm wooden battens, positioned evenly around the compartment (Figure 3.6b). The fire load was equivalent to 40kg of wood per square metre of floor area. Assuming a calorific value of 17.5MJ/kg for wood, the fire load density for the tested compartment was 700MJ/m^2. The fire load used was slightly higher than the office design fire load of 511MJ/m^2 (80% fractile) given in the EN1991-1-2. Each wooden crib was connected to its neighbour by a mild steel channel section, which contained a porous fibre board. Approximately 30min before ignition, 20 litres of paraffin was poured into the channels, to ensure rapid fire development within the compartment.

Instrumentation

Extensive instrumentation devices were placed throughout the compartment to measure the atmosphere temperatures, temperature distribution through the composite floor, the temperature of the protected and unprotected cellular beams, and the vertical and horizontal displacements. The locations of the measurements taken are shown in Figure 3.7 and Figure 3.8. A free-standing steel structure was built around the compartment to create a reference outer frame, allowing the correct measurement of vertical and horizontal displacements. A total of 350 thermocouples were used to monitor the temperatures and a total of 17 transducers were used to measure the various displacements. The transducers were attached to a free-standing outer reference frame and were insulated, where required, to ensure that and heat effects to the transducers were eliminated.

Under fire conditions the deflection of the unprotected, axially unrestrained, composite steel beams (Figure 3.9) predominately comprises two parts; thermal bowing and mechanical deflection. Deflection due to thermal bowing is caused by the non-uniform temperature distribution through the steel beam and the connected composite slab. The mechanical deflection is due to the decrease in stiffness and strength of the structural material as the temperatures increase. At low temperatures (less than 400°C), the beam deflection is predominantly due to thermal bowing. At higher temperatures, mechanical deflection will dominate and the deflection increases at a faster rate.

Figure 3.9: Developed compartment fire

Figure 3.10: Deflection of the slab/unprotected beam following the fire.

The maximum recorded steel temperature of 1053°C occurred after 77 minutes at the centre span of Beams 4 and 5 (Figure 3.11). The maximum temperature occurred on the bottom flange below the elongated opening. Figure 3.11 shows the temperature distribution at the critical part of the unprotected CBs. It is worth noting that the temperatures are non-uniform across the web despite the beams being unprotected and the long duration of the fire. The temperature of the top flange of the beams is lower, as expected, due to the heat sink effect of the supporting concrete slab. At a maximum temperature of 1053°C the steel has lost 97% of its strength and stiffness and is contributing little to the load bearing capacity of the floor system.
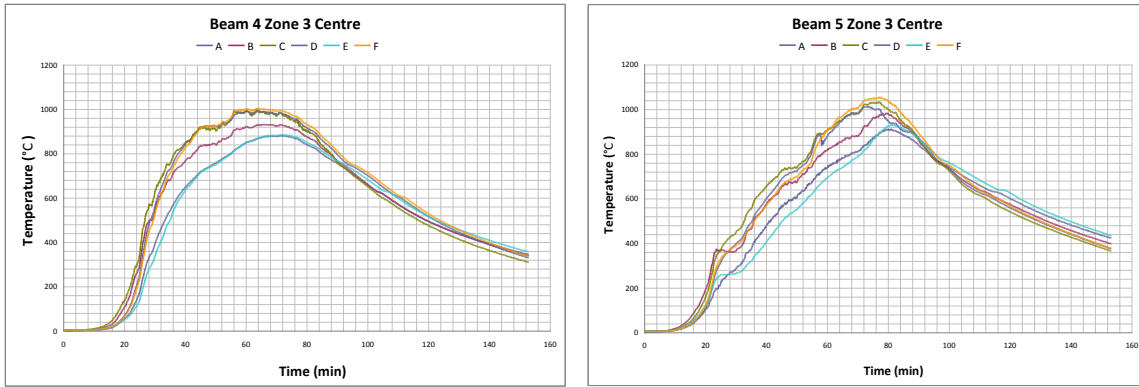
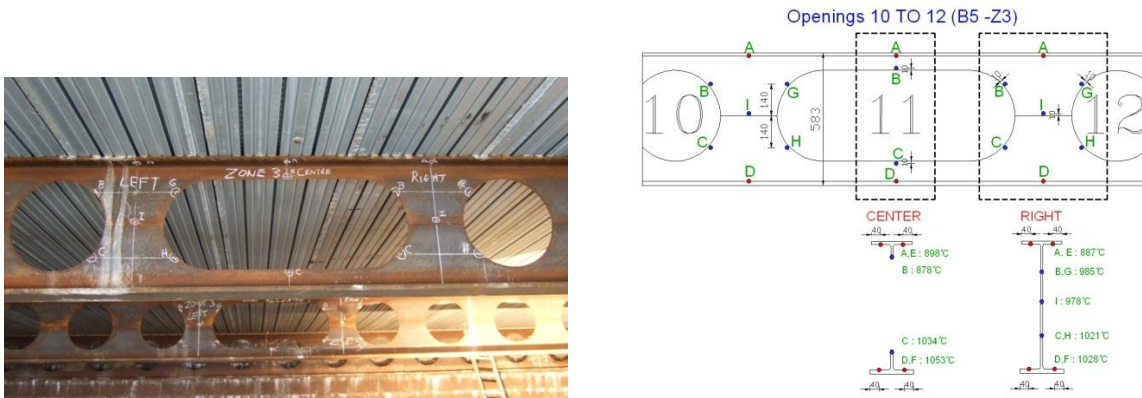Figure 3.11: Recorded temperatures at mid-span of the unprotected beams

Figure 3.12: Recorded maximum temperatures in the unprotected beams.

With increasing temperatures on the unprotected CBs (Figure 3.12), it was observed that post web buckling occurred initially. The composite action between the CBs and slab prevented twisting of the beam as a whole. The tendency for the bottom flange to displace laterally caused bending of the beam's web leading to overall distortional buckling, as shown in Figure 3.12. At this stage the unprotected steel temperatures were approximately 800°C and only the top flange was considered to be providing support to the slab by acting as a catenary. The temperature of the mesh reinforcement, above the beams reached a maximum of 375°C at 95 minutes, as shown in Figure 3.13 which was well into the cooling stages of the fire. Figure 3.14 shows the maximum recorded temperature of the mesh reinforcement between the beams, where again the maximum temperature occurred during the cooling stages of the fire. The temperature in the concrete slab continues to rise after the maximum atmosphere temperature, which occurred at 75 mins. The recorded temperatures of the shear studs are shown in Figure 3.15, where the maximum temperature reached 585°C. Although the shear stud temperature is high the amount of horizontal shear required reduces as the unprotected beams increase in temperature and lose strength and stiffness. There was no sign of loss of composite action of the beams suggesting that the shear studs performed adequately and maintained composite action between the slab and beams during the full duration of the test.
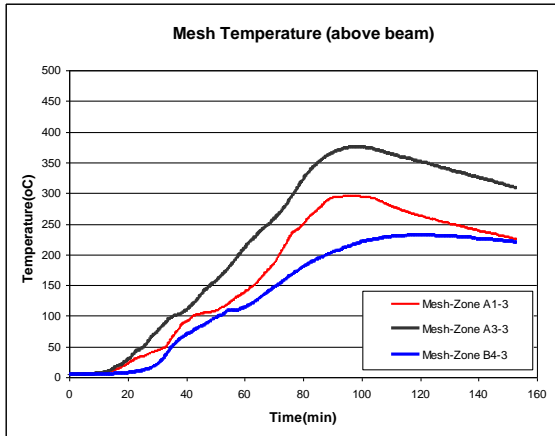
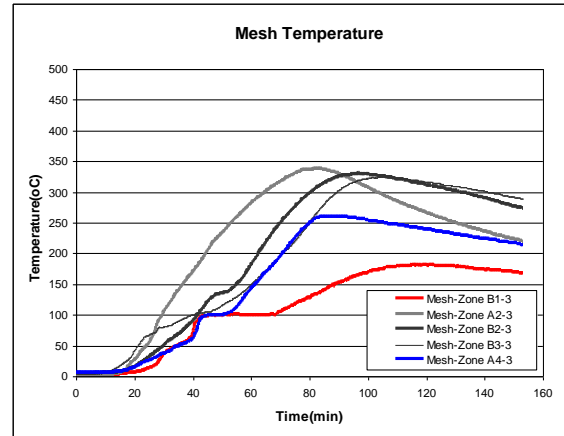Figure 3.13: Recorded temperatures of the mesh above the beams

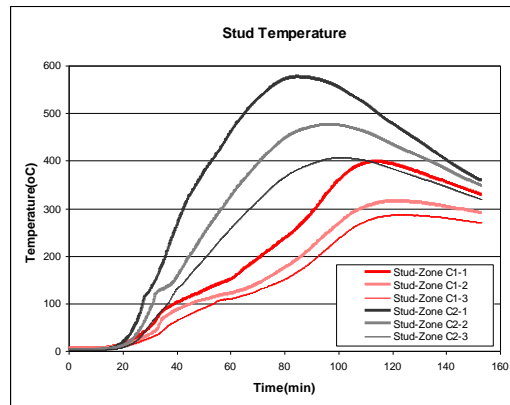Figure 3.14. Recorded temperatures of the mesh between beams

Figure 3.15: Recorded temperatures of the shear studs

The maximum recoded deflection of the slab was 783mm, which occurred after 112 minutes (Figure 3.16), which is well into the cooling stage of the fire. Figure 3.16 shows the time/displacement curve for Beams 4 and 5, during the test and after one day following the test. Figure 3.16 also shows the deflection after one month once the sandbags had been removed.
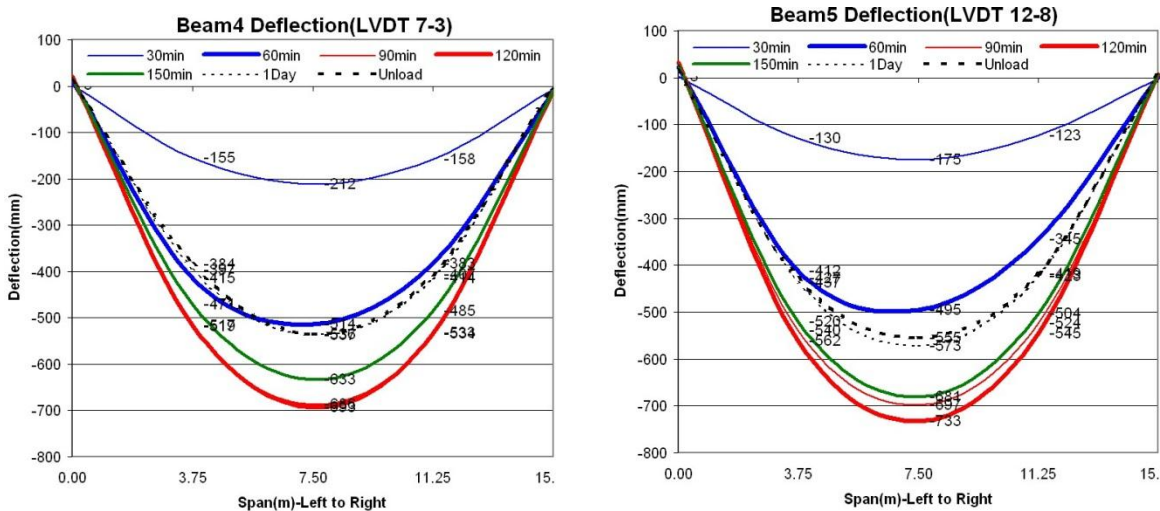

Figure 3.16: Deflection profile recorded on the slab/beam

The deflection profile of the floor slab, coupled with the composite action between the beams and slab, caused rotation of the top flange of the steel beam. This induced a secondary moment into the beam section, together with vertical shear force, leading to distortional buckling of the CBs driving the lower tee laterally out of its original plane. At this stage the load was predominately supported by membrane action of the floor slab, corresponding to fundamental principles outlined in the Bailey design method.

It can be seen that the unprotected cellular beams effectively went into catenary action, with only the top tee contributing to supporting the load. Web post buckling, which is commonly observed in isolated small-scale fire tests, occurred around the first opening in the beam where the overall displacements are restricted.

Membrane Action in Floor Slabs

The steel deck reached temperatures in excess of 900°C and was observed to have de-bonded from the concrete in most areas. At a temperature of 900°C the steel deck had lost 94% of its strength and therefore, coupled with de-bonding, did not significantly contributed to the overall strength of the floorplate at the point of maximum fire severity. This corresponds to the design assumption by Bailey where the contribution from the steel deck is ignored in the calculation of the load capacity of the slab. However, it is worth noting that the steel deck does have the beneficial effect of reducing the consequence of any spalling since it ensures that any spalled/cracked concrete stays in place, provided that the deck does not significantly debond and creates a large gap between the deck and concrete. In the test a large crack occurred across the short span of the floor slab (Figure 3.17) corresponding to the previous test observations of membrane action.
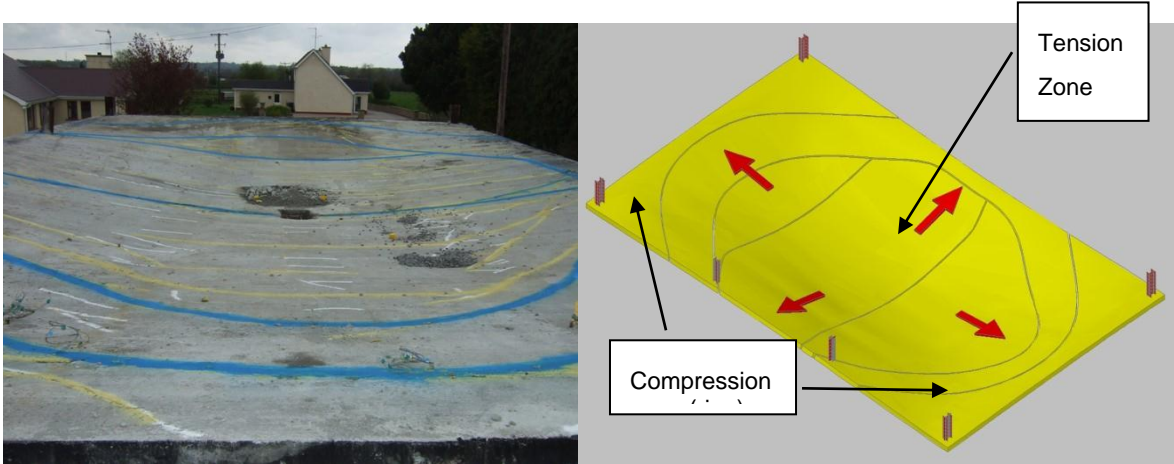

Figure 3.17. Cracking pattern highlighting behaviour of the slab

The supported concrete slab was not horizontally restrained around its perimeter and the supporting protected perimeter beams maintained their load carrying capacity and were subjected to small vertical displacements. This allowed membrane action to develop with the in-plane forces in the central region of the slab going into tension and in-plane equilibrium compressive forces forming in the slab around its perimeter (Figure 3.17). This behaviour is analogous to a bicycle wheel; the spokes representing tensile membrane action, and the rim representing compressive membrane action.

Conclusions

The floorplate performed extremely well supporting the applied load for the duration of the test and highlighted the inherent strength in the system due to membrane action of the floor plate. Based on the measured data it was shown that the reinforcement in the central region of the slab was under tensile force forming an elliptical parabolic tensile mesh anchored by a concrete compressive ring forming around the perimeter of the slab. Due to membrane action, the existence of secondary beams to support the slab is not necessary in the fire condition and these beams can be left unprotected.

Acknowledgements

About the authors *JÁRMAI, Károly, University of Miskolc, Hungary, VASSART, Olivier, ArcelorMittal Esch, Research and Development, Luxembourg, ZHAO, Bin, CTICM –Fire and Testing Division, France*

3   REFERENCES

1.   *'Fire Safe Design: A new approach to multi-storey steel framed buildings' P288, The Steel Construction Institute, 2006.*

2.   *'The behaviour of Multi-storey steel framed buildings in fire', A European joint research programme, British Steel Swinden Technology Centre, 1999*

3.   *Lennon, T., 'Cardington fire tests: instrumentation locations for large compartment fire test.', Building Research Establishment Report N100/98, June 1996.*

4.   *Lennon, T., 'Cardington fire tests: instrumentation locations for corner fire test.', Building Research Establishment Report N152/95, June 1996*

5.   *Bailey C.G. and Moore D.B., The structural behaviour of steel frames with composite floor slabs subjected to fire: Part 1: Theory*

6.   *Bailey C.G. and Moore D.B., The structural behaviour of steel frames with composite floor slabs subjected to fire: Part 2: Design*

7.   *Hayes B. and Taylor R. Load-Testing RC slabs. The Consulting Engineer. Nov. 1969. pp 46-47*

8.   *Taylor R., Maher D.R.H. and Hayes B. Effect of arrangement of reinforcement on the behaviour of the reinforce concrete slabs. Magazine of concrete research Vol 18 No. 55. June 1966. pp 85-94*

9.   *Bailey CG, Membrane action of slab/beam composite floor systems in fire. Engineering Structures 26 2004:1691-1703.*

10. *Sawczuk A. and Winniki L. Plastic behaviour of simply supported reinforced concrete plated are moderately large deflections. Int J. Solids Structures Vol 1 1965 pp. 97 to 111.*

11. *EN 1992-1-2, Eurocode 2, Design of concrete structures. Part 1.2: General rules. Structural fire design, CEN*

12. *EN 1994-1-2, Eurocode 2, Design of composite steel and concrete structures. Part 1.2: General rules. Structural fire design, CEN*

13. *EN 1994-1-1, Eurocode 4 Design of composite steel and concrete structures – Part 1-1: General rules and rules for buildings, CEN*

14. *EN 1993-1-8, Eurocode 3 Design of steel structures – Part 1-8: Design of joints, CEN*

15. *EN 1992-1-1, Eurocode 2 Design of Concrete Structures – Part 1-1: General rules and rules for buildings, CEN*

16. *EN 1991-1-2 - Eurocode 1 " Actions on structures. General actions. " – Part 1-2: Actions on structures exposed to fire, CEN.*

17. *Vassart, O. and Zhao, B. "Fire Resistance Assessment of Partially Protected Composite Floors (FRACOF) Design guide", Leonardo Da Vinci European Program, 2009.*

18. *Vassart, O. and Zhao, B. "Fire Resistance Assessment of Partially Protected Composite Floors (FRACOF) Engineering Background", Leonardo Da Vinci European Program, 2009.*